# Study of density and orientation in poly(ethylene terephthalate) using Fourier transform Raman spectroscopy and multivariate data analysis

**N. Everall*, P. Tayler, J. M. Chalmers and D. MacKerron**
*ICI plc, Wilton Materials Research Centre, Wilton, Middlesbrough, Cleveland TS6 8JE, UK*

**and R. Ferwerda and J. H. van der Maas**
*Department of Analytical Molecular Spectrometry, University of Utrecht, PO Box 80083, 3508 TB Utrecht, The Netherlands*
*(Received 8 October 1993; revised 3 December 1993)*

Partial Least Squares modelling techniques have been used to calibrate Raman spectra in terms of the density of poly(ethylene terephthalate), with a standard prediction error of 0.0024 g $cm^{-3}$. The calibration, which utilizes, primarily, the bands at ~1730, 1094, 997, and 860 $cm^{-1}$, spans isotropic, uniaxial and biaxially oriented samples with a single model; this is superior to univariate calibrations which require separate models for isotropic and oriented samples. Hierarchical Cluster Analysis and Principal Components Analysis were also used for exploratory analysis of the spectra; these methods grouped samples in terms of their density and orientation characteristics, and also identified the bands which responded most significantly to morphology changes. It was shown that the 1615 $cm^{-1}$ ring-stretching mode differentiated the samples on a basis other than simply by density or orientation alone; further work, however, is needed to understand this behaviour. The potential power of multivariate analysis techniques for correlating Raman spectra and polymer morphology was clearly demonstrated.

**(Keywords: poly(ethylene terephthalate); density; Raman)**

## INTRODUCTION

### *General*

The infra-red (i.r.) and Raman spectra of poly(ethylene terephthalate) (PET) have been discussed in a number of papers[1–4], with particular regard to the influence of the morphology of the material. X-ray diffraction and infra-red studies of PET have demonstrated that the ethylene glycol units have a *trans* structure in the crystalline state, while the amorphous state possesses primarily the *gauche* structure[1,2]. However, Lin and Koenig[3] showed that the *trans* conformer can also exist in the amorphous phase, and have determined differing densities for the *gauche*, amorphous *trans* and crystalline *trans* conformers. This work was supported by the Raman observations of Adar and Noether[4], who proved that spin-oriented fibres could be prepared with a high level of molecular orientation and an increase in *trans* conformer content, but without any significant crystallization, as judged from X-ray diffraction data. In particular, they showed that the bands at 1000 and 1096 $cm^{-1}$ should be associated with the *trans* conformer of the glycol unit and so are not directly indicative of increasing crystallinity. Also importantly, they confirmed that the decrease of the carbonyl stretching mode bandwidth (as first demonstrated by Melveger[5]) was a reliable indicator of an increase in crystallinity, since this narrowing is strictly associated with a true increase in the amount of the crystalline phase (as measured by X-ray diffraction), rather than simply intramolecular conformation changes. A linear correlation between density and C=O bandwidth has been proposed and has been used to infer changes in crystallinity[5].

The above work illustrates the importance of distinguishing between the effects of chain conformation (intramolecular) and those of chain packing (intermolecular). In addition, care must be taken when analysing oriented PET by Raman spectroscopy since the relative orientations of the molecular axes and the laser electric vector influences both the relative band intensities within the spectrum[4] and the C=O bandwidth[6]. Therefore, a calibration used for determining crystallinity which has been obtained solely from isotropic standards may well be invalid when applied to samples showing overall molecular orientation. It is therefore clear that the problems of differentiating the effects of crystallinity, conformation and orientation can make it a non-trivial task to derive the crystallinity of the samples from the i.r. or Raman spectra. This is further complicated if one is not measuring crystallinity directly by using X-ray scattering, but rather uses another (simpler) parameter (e.g. density or d.s.c. measurements) which one then hopes to correlate with crystallinity. The success of this approach depends on the complexity of the system; if a simple two-phase system (amorphous/crystalline) is under study, and the densities of the

*To whom correspondence should be addressed

0032-3861/94/15/3184-09

amorphous and crystalline phases are known, then the crystallinity can indeed be calculated from the density of the sample. However, if more than two phases are present this simple calculation is inappropriate, although the density itself may still be a useful parameter to measure and will be expected to increase with increasing crystallinity.

For industrial purposes, such as those of interest in our laboratory, measurement of the density is often an acceptable alternative to crystallinity for characterizing the influence of process conditions on final product properties, although a detailed understanding of polymer microstructure is not obtained when using this approach. Once established, vibrational spectroscopic calibrations for density or crystallinity will often be preferred to direct measurements, since they are quicker to apply in practice, and allow the morphology to be measured under difficult conditions, such as mapping (on the micrometre scale) through polymer components[6]. Accordingly, for the purposes of these studies, the sample density was used as the primary calibration standard, rather than the percentage crystallinity, which is more difficult to measure directly. Given the results of Adar and Noether[4] this method will also yield an *indication* of changes in the crystalline content, since the C=O band only narrows in the true crystalline regions.

Raman methods have been frequently used to study PET morphology[4–7]. In conventional Raman spectroscopy using visible excitation, the spectra of industrial-grade polymers often suffer from intense fluorescence, usually caused by impurities or degradation. Therefore, poor spectra are often obtained or long measurement times can be necessary. Because of the variable fluorescence background, the application of Chemometrics, in which, by means of computer-based statistical methods, correlations between spectra and properties of the material are found, is made more difficult. Fourier transform (near infra-red) (*FT*(n.i.r.)) Raman spectroscopy avoids most of the problems of fluorescence, and often generates good signal-to-noise (S/N) spectra with constant, low backgrounds, which are suitable for subsequent multivariate analysis.

The aim of this present study was to obtain good quality Fourier transform (*FT*) Raman data from PET samples exhibiting a range of densities and degrees of orientation, and to apply Chemometrics methods to produce a robust calibration for density which is independent of the degree of orientation. Simple univariate 'manual' calibrations were also performed for comparison. In addition, pattern recognition techniques and factor analysis were used to discern oriented and isotropic samples from their Raman spectra, and to identify the spectral features which prove most effective in the calibration model. We believe that this is the first reported use of Chemometrics to analyse the morphology of PET using Raman data.

### *Chemometric analysis*

Chemometric pattern recognition and calibration techniques were used for analysis of the Raman data. These multivariate methods provide a rapid and convenient way of identifying and quantifying systematic changes in data sets, including peak shape changes and combination effects throughout the spectra, which can then be associated with known physical differences between the samples. Traditional univariate calibration methods require a single, independent peak which correlates directly with the property of interest; this approach is often inadequate because of severely overlapped bands or complex correlation relationships.

In the present study, two approaches were adopted. First, an exploratory (unsupervised) analysis was carried out by using Principal Components Analysis (PCA) and Hierarchical Cluster Analysis (HCA). These approaches have been discussed in detail elsewhere[8–11] and this background will not be repeated here, except to note that both are data reduction techniques which give a simplified overview of trends in data sets. HCA classifies spectra on the basis of their similarity, thereby 'grouping' like samples, while Principal Components (PCs) are orthogonal basis vectors which seek to model the variation in a data set as fully as possible. Any spectrum can then be classified in terms of its PC 'scores', i.e. the PCs act as coordinates to describe the spectrum in multivariate data space. The advantage is that while a spectrum may consist of several thousand data points, only a few PCs are typically required to summarize most of the variations within a sample set. Furthermore, the spectral variables which contribute most to a given PC can be identified, and so sometimes physical or chemical significance can be attached to the results over and above a simple classification. Therefore while HCA gives a simple graphical display of sample similarity, PCA indicates which spectral variables are most important in differentiating samples.

Quantitative calibration was carried out using Partial Least Squares (PLS) modelling. This technique also reduces complex spectral variations to a few factors which can be correlated with quantitative changes (density, in this work) in a calibration sample set. This produces a model which can then predict the composition of unknown samples from their spectra. PLS, and other calibration models, have been discussed in detail elsewhere[10,11].

## EXPERIMENTAL AND ANALYSIS

### *Sample preparation*

Samples of isotropic PET chips (ICI) were heat-crystallized by annealing in an oil bath at different temperatures for various lengths of time. Uniaxially and biaxially drawn films of different draw ratio and annealing conditions were used to provide oriented samples with differing densities. Details of the sample preparation are given in the Appendix. Sample densities were measured by using a density column, taking an average of the results obtained for five different chips (each of ~30 mg mass). Standard errors were of the order of 0.0002 g $cm^{-3}$.

### *Instrumentation*

*FT*(n.i.r.) Raman spectra were recorded on a Perkin–Elmer 1760 FTIR spectrometer, equipped with a Raman module and an InGaAs detector which was operated at 77 K in order to obtain a high S/N ratio. Samples were excited by the 1064 nm line of a polarized Nd:YAG Spectron SL301 laser. All spectral data were collected with a resolution of 2 $cm^{-1}$, using a measurement time of 11 min (40 scans). To avoid induction of crystallization, a maximum of 200 mW laser power was used. Significantly higher powers (e.g. 1 W) were found to crystallize the PET in some cases.

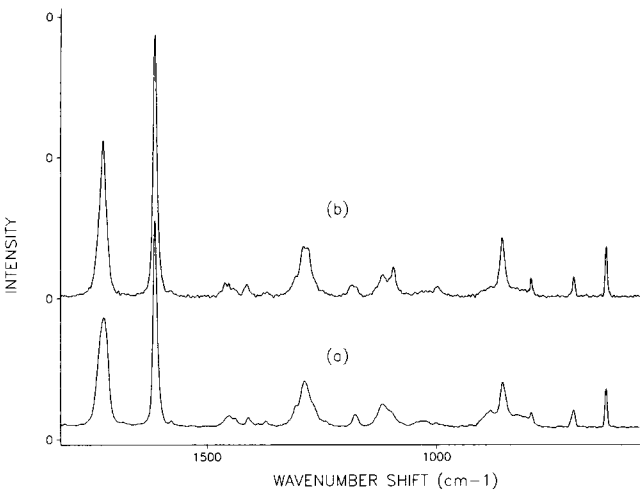


**Figure 1** *FT* (n.i.r.) Raman spectra of PET: (a) virgin chip; (b) annealed for 2 h at 150°C. Note that several bands change in relative intensity

No sample preparation was necessary, and samples were mounted directly in the laser beam (~1 mm spot size). Backscattered radiation is collected with this particular instrument. In the case of oriented films, all spectra were obtained with the laser beam polarized parallel to the forward draw direction of the film. No polarization analyser was used. After optimization of the sample holder position, all spectra were recorded under fixed alignment conditions, to minimize any potential differences caused by self-absorption of the Raman scatter by the sample[12,13].

*Data preprocessing and analysis*

All chemometric processing was carried out using the Pirouette software package (Infometrix Inc., USA). The spectral region 1800–600 $cm^{-1}$ was used in this work, since it was found to contain all of the major peaks of interest. It was found that data could be grouped at 8 $cm^{-1}$ resolution without reducing the accuracy of the calibration, implying that spectra could be collected more rapidly at lower resolution without degrading the calibration precision. All spectra were normalized to a constant total area over the spectral region in order to compensate for variations in laser intensity and alignment between samples. This removes the effect of absolute intensity variations and focuses on relative differences between the spectral features.

## RESULTS AND DISCUSSION

*Univariate analysis*

The spectra that were obtained showed a high S/N ratio (*Figure 1*), although the efficiency of the Raman scattering is decreased by a factor of 23–56 when compared to excitation with the 488 nm line of an argon laser, due to the $\sim\nu^4$ dependence of the scattering process[14]. However, the main benefit of the n.i.r. excitation is apparent when the conventional spectra (488 nm excitation) of virgin and annealed PET chips are examined (see *Figure 2*). While the virgin chip gave a good, low-background spectrum, the annealed chips gave rise to an intense fluorescent background which lowers the spectral S/N and potentially distorts the band shapes. The fluorescence can be minimized by annealing the virgin samples under dry air, which implies that products of hydrolysis gave rise to the background. No fluorescence was generated using n.i.r. excitation, which is a clear advantage for this type of quantitative work.

Melveger[5] has previously correlated a narrowing of the 1730 $cm^{-1}$ C=O stretching band with increasing PET density. This has been rationalized on the basis of increasing coplanarity of the C=O and aryl moieties in the crystalline regions, giving a smaller range of C=O environments and hence a narrower band. Our measurements of the C=O bandwidths of these PET chip samples confirmed Melveger's *general* findings, but we did not observe a simple *linear* decrease in bandwidth with increasing density (see *Figure 3*, curve (a)). In addition, we found that the correlation for the oriented samples (*Figure 3*, curve (b)) did not exactly overlap that for the isotropic chips; thus it is necessary to make assumptions about, or measurements on, sample orientation prior to deducing sample density from the C=O bandwidth. The same effect was observed when it was attempted to utilize

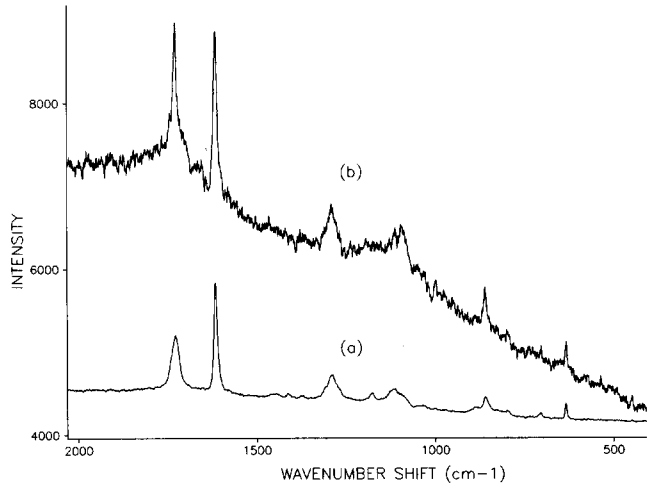


**Figure 2** Conventional Raman spectra of PET: (a) virgin chip; (b) annealed for 2 h at 150°C. Conditions: 488 nm excitation (50 mW); 5 min acquisition time; Dilor XY spectrometer with intensified diode array detector. Note the intense fluorescent background from the annealed chip

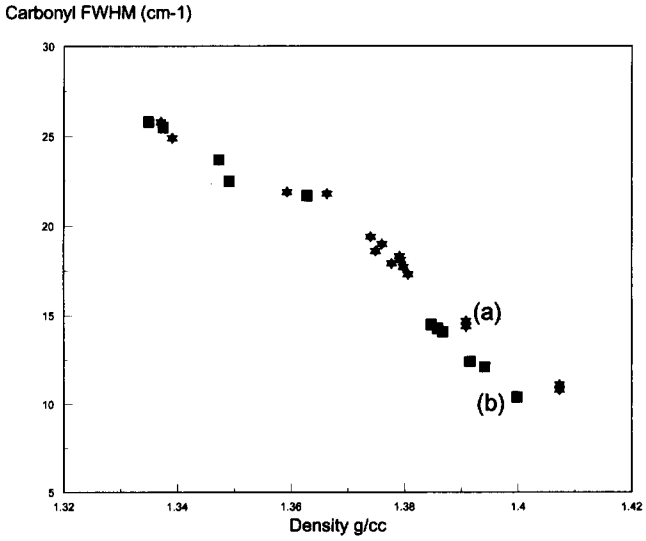


**Figure 3** Relationship between carbonyl stretching bandwidth and density of PET samples, for (a) isotropic chips (*) and (b) oriented films (■). Note that the (oriented) film samples require a different correlation curve

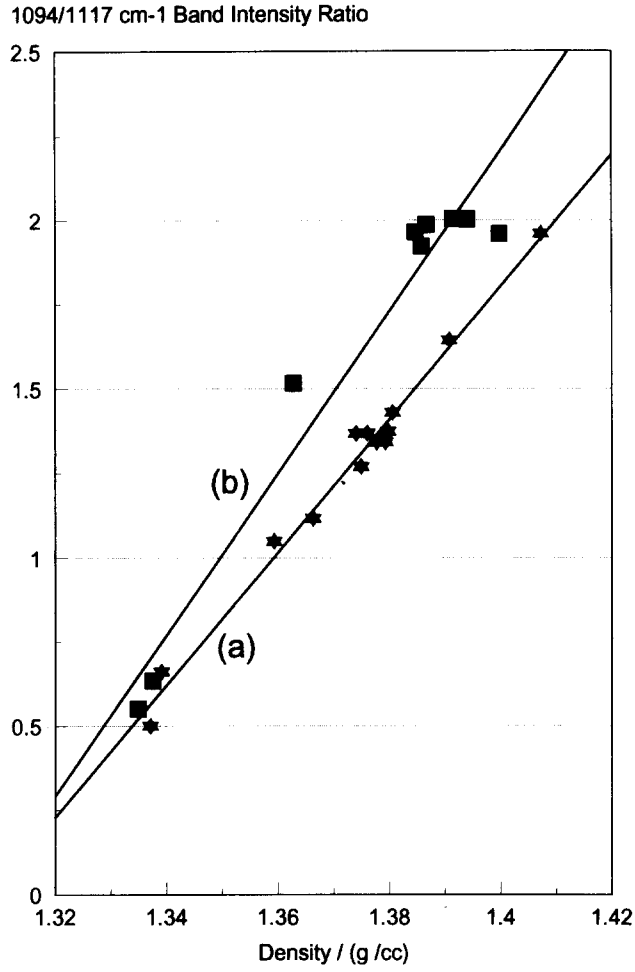


**Figure 4** Correlation of the 1094 $cm^{-1}$ band intensity (normalized to the 1117 $cm^{-1}$ band) with PET density, for (a) isotropic chips (*) and (b) oriented films (■). Note the influence of molecular orientation on the correlation curve

the 1094 $cm^{-1}$ band intensity as a measure of sample density (*Figure 4*); although good correlations for the isotropic and oriented sample sets could be obtained independently, it was not possible to produce one model which could analyse all samples irrespective of orientation. This is in agreement with the observations of Melveger[5].

As Adar and Noether[4] stated, Raman spectra are influenced by chain conformation, chain packing and the orientation of the polymer axis in anisotropic samples. Although several bands were observed to vary upon annealing (see *Figure 1*), they concluded that only the 1182 $cm^{-1}$ band seems to be a true crystallinity band, i.e. arising from three-dimensional ordering rather than conformational changes. Because our sample set contains both isotropic and oriented polymers with a range of densities, the differences in the spectra can arise from all of the factors noted above, hence it is not surprising that the simple univariate calibrations in *Figures 3* and *4* were unable to span all samples in a simple calibration against density.

*Multivariate calibration*

HCA (single-link clustering) and PCA were applied to the entire sample set for a preliminary qualitative analysis. *Figure 5* shows the HCA output in the form of a dendrogram, which organizes samples into clusters based upon their degree of similarity. This gives a simple visual classification of the samples based solely upon the Raman data. From *Figure 5*, two main groupings are obvious. The upper half (PET 52–PET 44) contains samples which are oriented, and also three isotropic samples (ob25, ob21 and ob42) of low density. Within this grouping, two subgroups can be identified; the first of these (PET 52–PET 43) contains samples with densities below 1.37 g $cm^{-3}$, while members of the other set (PET 49–PET 44) all have densities in excess of 1.38 g $cm^{-3}$. Further subdivisions exist which differentiate chips and film samples, although, for example, samples ob21, ob25 and PET 52 are very similar, since they are all of low density, and PET 52 is of low orientation, as judged by birefringence measurements.

The main lower grouping (ob43–ob24) contains only isotropic samples. Two subgroups can be identified but these cannot currently be rationalized on the basis of a known physical property. Sample ob00 is a distinct outlier (it occupies its own branch); this was an amorphous chip which underwent no annealing. It is obviously dissimilar to all of the other samples, even though several others were also of low density. Because it was unrepresentative of the sample set in terms of its preparation, it was excluded from the subsequent analyses reported below, although in fact it was found that its density could actually be predicted adequately by the PLS calibration model formed by using the remaining samples.

It is apparent that HCA is a good preliminary method for classifying the PET samples, particularly in terms of

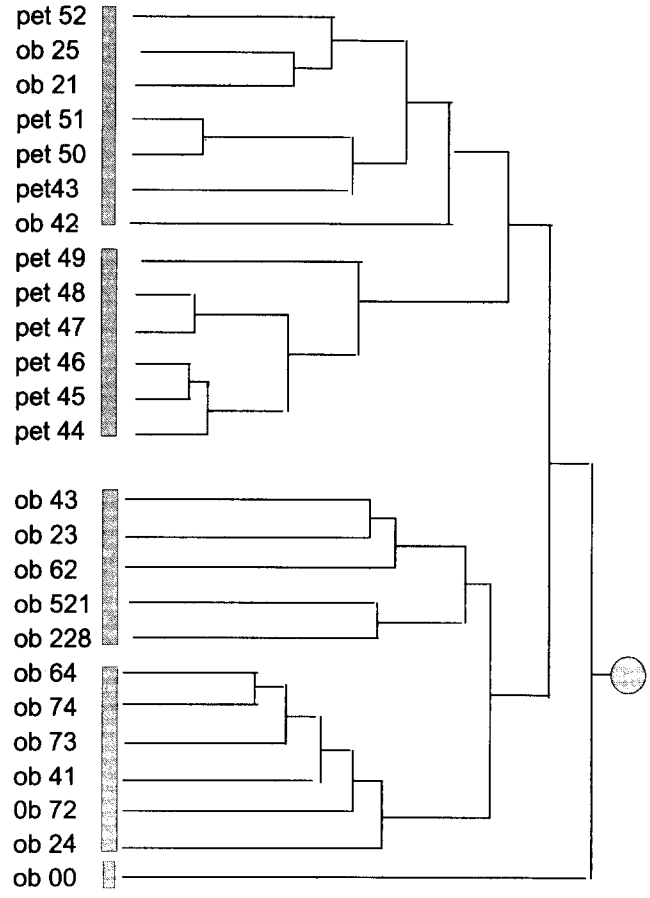


**Figure 5** Dendrogram resulting from HCA of a full PET sample set, with sample clustered in terms of spectral similarity. The virgin chip (ob00) is a clear outlier

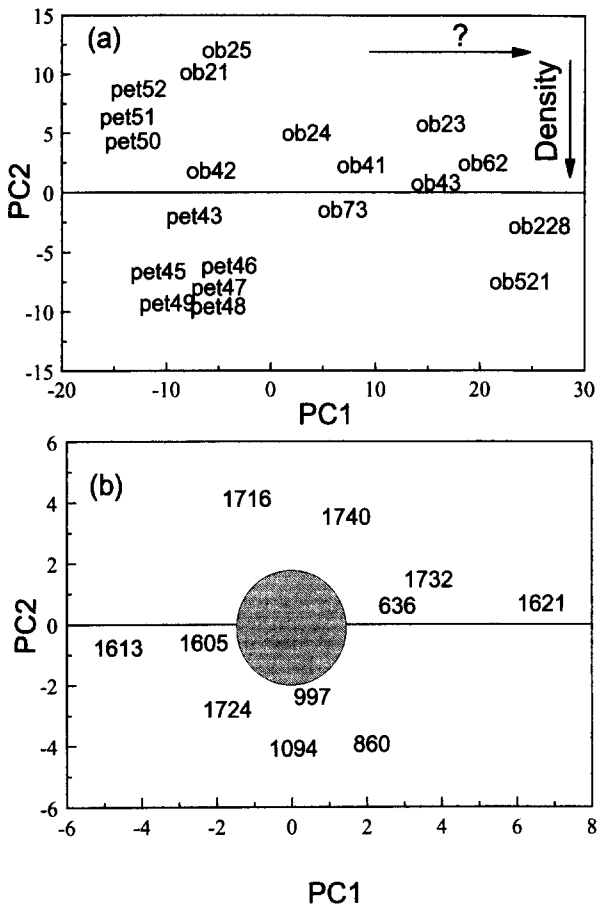


**Figure 6** Results of PCA analysis of a full PET sample set (minus ob00): (a) scores plot; (b) loadings plot. Some samples have been excluded from the *output* on the scores plot (and also those in *Figures 8* and *10*) to avoid overlap of identifiers. The numbers on the loadings plot represent the wavenumber shifts which load most heavily into PC1 or PC2, i.e. the positions in the spectra which show most variation through the sample set. The shaded area at the centre of each plot represents an area of dense overlap of many points, none of which load significantly into PC1 or PC2, and hence are not shown individually for the sake of clarity

isotropic and oriented material, and the effects of density can also be discerned to some extent. However, for a more detailed exploration of the data, PCA is a more suitable approach.

*Figure 6* shows the results of the PCA of the same sample set (excluding ob00). It was found that PC1 and PC2 accounted for ~66 and 23% of the total variance, respectively. The scores plot (*Figure 6a*) confirms that the oriented, more dense samples formed a separate group, as did the uniaxial films. Comparing the scores and the loadings (*Figure 6b*) plots, we see that PC2, and hence variations in the 1730, 1094 and 860 $cm^{-1}$ bands, correlate with increasing density, while the ring stretching mode at 1615 $cm^{-1}$ dominates PC1 and is presumably the main reason for the distinction between the high-density films (PET48 and PET49) and high-density chips (ob521 and ob228). The chip set itself is widely dispersed along PC1 (not in order of density) and so clearly the 1615 $cm^{-1}$ band is important in distinguishing their spectra. The 1615 $cm^{-1}$ band is known to be sensitive to orientation[15] (hence the differentiation between chip and film data), but this cannot be the discriminating factor within the chip set. Repeating the PCA analysis using *only* the chip set (results not shown here for the sake of brevity) gave very similar results; the 1615 $cm^{-1}$ band loaded heavily into a PC which obviously could not represent orientational differences, and which did not differentiate between samples on the basis of density either! It is not clear at this stage why this band is important in distinguishing between the isotropic samples; this feature will be investigated in future studies. It can be seen that the distinction between density and conformational changes is an obvious area for closer study.

Since we are primarily interested in the study of density, it was decided to remove the 1615 $cm^{-1}$ band from the analysis. The rationale for this was to try to enhance the discrimination in terms of density and to minimize the effects of sample orientation or other factors which might influence the 1615 $cm^{-1}$ band intensity. Both HCA and PCA were repeated with the data range from 1650–1500 $cm^{-1}$ excluded from the analyses. The resulting dendrogram from the HCA is shown in *Figure 7*. Two main groups were found; with the exception of PET 43 (the lowest density biaxial film), the dense, oriented samples formed a separate cluster (PET 49–PET 44), while there was comparatively little distinction between the other chip and film samples, other than a small subgroup of low-density materials (PET 52–PET 50). The scores plot from the PCA (*Figure 8a*) now shows (a) that PC1 primarily differentiates samples on the basis of density, with the most dense samples having large negative scores, and (b) the oriented films all have large negative PC2 scores. PC1 and PC2 accounted for 49 and 36% of the variance, respectively. Again, it is unclear as to why the isotropic chip samples are dispersed along the PC2 axis, but this shows that PC2 cannot solely

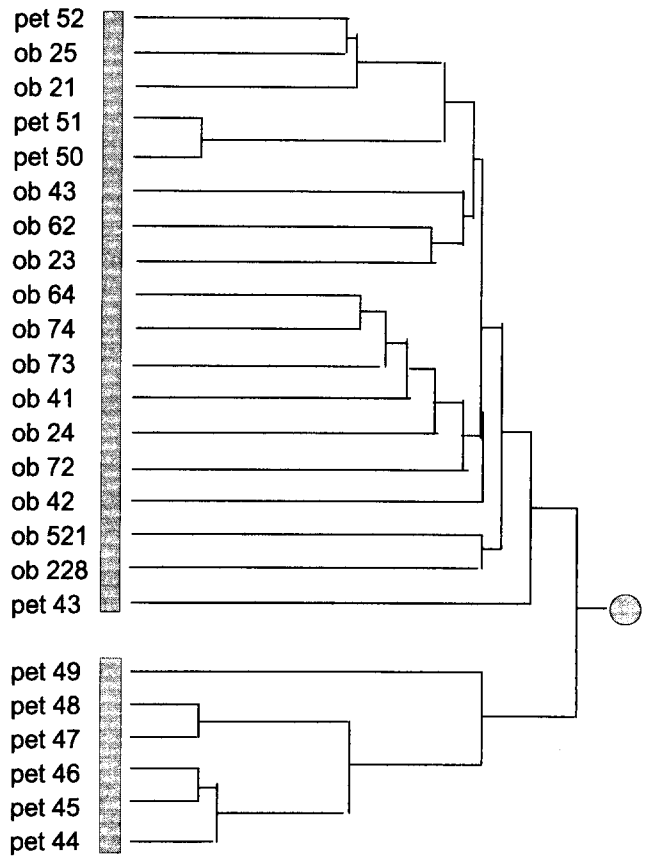


**Figure 7** Repeat of HCA on a PET sample set with the 1615 $cm^{-1}$ band excluded

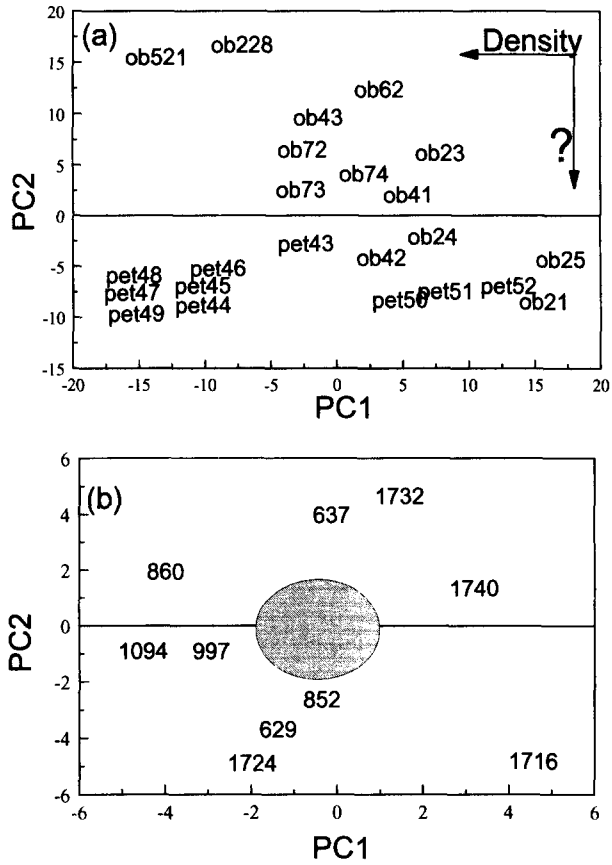


**Figure 8** Repeat of PCA on a PET sample set with the 1615 $cm^{-1}$ band excluded: (a) scores plot; (b) loadings plot. Note the strong influence of density on PC1. Although oriented films all have a large negative PC2, so also do the low-density chips; clearly PC2 does not respond solely to orientation (see text for details)

represent differing levels of orientation. Significantly, eliminating the 1615 $cm^{-1}$ region has increased the sensitivity of the model to changes in density, i.e. the PC representing changes in density now accounts for nearly half of the total variance, as opposed to only 23% in the previous model. This is valuable information for the construction of a *quantitative* calibration model.

A parameter other than orientation must be important in influencing PC2; one factor is that the samples with large positive PC2 scores have all been heated at elevated temperatures for extended periods of time, and might be expected to have the more perfect three-dimensional ordering of molecules. Perhaps PC2 distinguishes between three-dimensional packing effects and intramolecular conformational changes. Another possibility is that PC2 responds to chemical and spectral changes induced by sample degradation (which would be expected to increase with heat setting temperature and time). Further work is in hand to try to understand the differences which are observed here; specifically, *trans/gauche* glycol conformer ratios will be examined using Raman data[4] to try to distinguish the differences in intramolecular conformations in the sample set, since as was noted in the Introduction, both *inter-* and *intra*-molecular changes can influence the spectra and densities.

The loadings plot (see *Figure 8b*) indicates that a simultaneous decrease in intensity at 1716, 1732, and 1740 $cm^{-1}$, coupled with an increase in intensity at 1724, 1094, 860, and 997 $cm^{-1}$, correlates with increasing density (i.e. the C=O bandshape changes and band intensity increases at 1094, 997, and 860 $cm^{-1}$). This is in good agreement with the changes seen in *Figure 1*. It should be remembered that the 1094 and 997 $cm^{-1}$ bands are associated with the *trans* conformer of the glycol unit, rather than with the crystalline phase *per se*, and so the analysis confirms the observation that the *trans* conformer is more prevalent in the crystalline phase[4].

Only qualitative information can be derived from this exploratory analysis alone; it is of interest now to turn to the quantitative calibration results. A PLS calibration model was first formed, using the full sample set, to relate spectra and densities. Normalization and mean-centring of all data was carried out prior to analysis, and full cross-validation was performed to optimize the number of factors used in the model (chosen to minimize the Predicted Residual Error Sum of Squares (PRESS)[11]). Variance scaling was not used as this reduced the prediction accuracy of the resultant model. It was found that a better model was produced when the 1615 $cm^{-1}$ band was excluded from the calibration, implying that it is not simply related to sample density. This supports the conclusions drawn from the PCA method.

*Figure 9* shows the cross-validated prediction plot for a PLS model optimized with four factors. The standard error of prediction (SEP) for the model was 0.0024 g $cm^{-3}$. This compares favourably with the SEP for a model obtained using the full spectrum (i.e. including the 1615 $cm^{-1}$ band) which was 0.003 g $cm^{-3}$. The scores

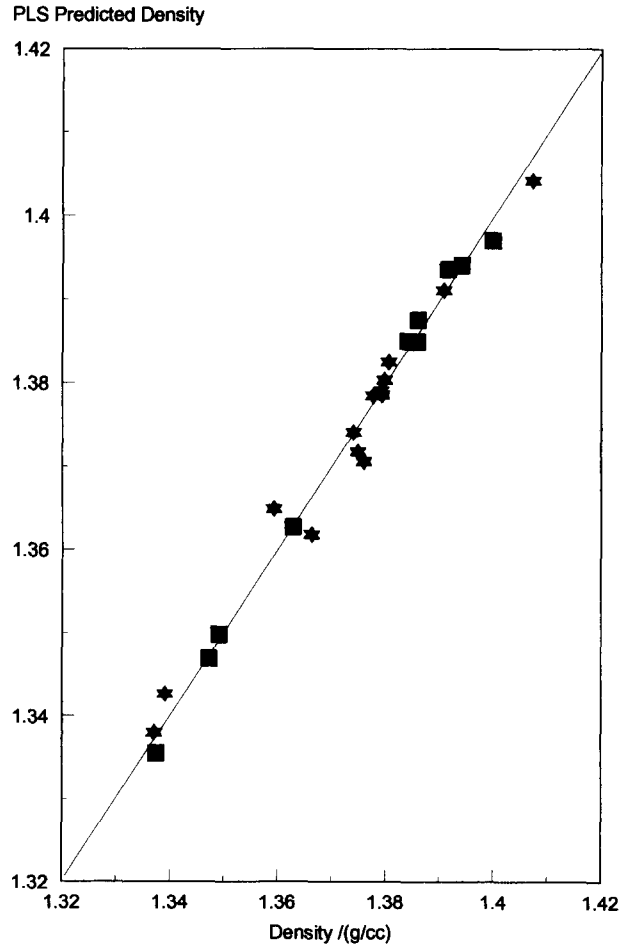


**Figure 9** Cross-validated prediction plot for PLS calibration using a full PET sample set and four factors (SEP = 0.0024 g $cm^{-3}$): (*) chips; (■) film samples. Note that the isotropic and anisotropic samples can readily be included in the same model (in contrast to *Figures 3* and *4*)

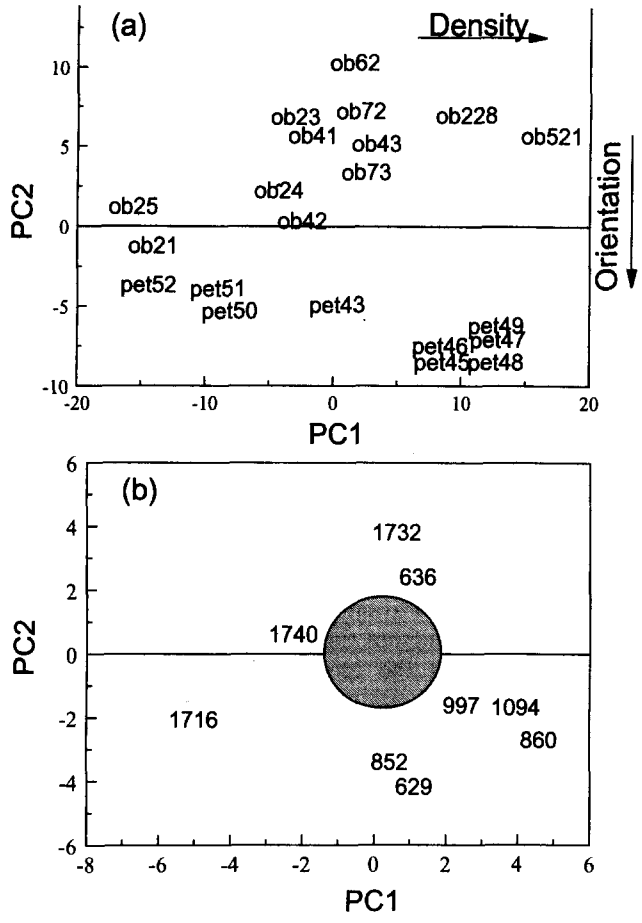


**Figure 10** Results of a PLS analysis of a full PET sample set: (a) scores plot; (b) loadings plot. Note that factor 1 essentially models variation in density, while factor 2 distinguishes chip and film samples (orientation); factor 2 also differentiates the chips to some extent; so orientation cannot be the sole influence

plot for the PLS model (*Figure 10a*) shows that the first factor essentially distinguishes density, whereas the second factor differentiates samples primarily on the basis of orientation (although the chip spectra are also dispersed along the second factor to some extent, implying that the effects observed in *Figure 8* also have some influence on the PLS model). Factors 1 and 2 accounted for 47 and 22%, respectively, of the variance in this model. The loadings plot (*Figure 10b*) reveals that the C=O band and bands at 1094, 997, and 860 $cm^{-1}$ are primarily used in predicting density, whereas the C=O and the ~630 and 860 $cm^{-1}$ bands contribute most strongly to factor 2 (orientation), in broad agreement with the PCA results discussed above. This is not surprising, since although the PLS factors are constructed to form the best predictive model, they are expected to be similar to the components generated by the PCA. However, the most important point from this work is that the PLS calibration allows one to analyse isotropic or oriented samples using the *same* model; the data for the film samples cannot be discerned from those for the chips in *Figure 9*, in contrast to the results shown in *Figures 3* and *4* for univariate calibration.

It is of interest to compare the PLS model which spans the entire sample set with those which can be produced using either isotropic or drawn sample sets in isolation. *Figures 11* and *12* show cross-validation plots for four-factor models for the isolated chip and film data sets, respectively. The respective SEPs were 0.0022 and 0.0023 g $cm^{-3}$. The SEP for the complete model (*Figure 9*, 0.0024 g $cm^{-3}$) is only slightly degraded when compared to those of the models optimized for chip or film sets individually; therefore, there is no practical advantage in using two separate models for calibration, in sharp contrast to the uniaxial models, where this is essential (see *Figures 3* and *4*). As would be expected, one cannot use the 'chip-only' model to predict densities for the oriented sample set (*Figure 13*); this results in anomalously high predictions of density in the same way that the univariate, isotropic sample calibrations fail when applied to oriented samples (*Figures 3* and *4*). This illustrates the necessity of incorporating a sufficiently wide range of calibration samples when forming the working model.

Finally, it was found that an effective calibration could be formed even when only bands below 1340 $cm^{-1}$ were used; in this case a five-factor model was required to minimize the PRESS, and gave a SEP of 0.003 g $cm^{-3}$. Therefore, even when the most traditional 'manual' calibrator for density, namely the C=O stretching band, was eliminated, a valid model could still be formed which spanned both isotropic and oriented material. (In contrast, simple univariate calibrations using bands in this region were wholly inadequate, for example, the 1094 $cm^{-1}$ band was sensitive to orientation (*Figure 4*), and the 860 $cm^{-1}$ band intensity did not correlate with the density of either chip or film samples (data not shown here).) However, we must remember that these bands are

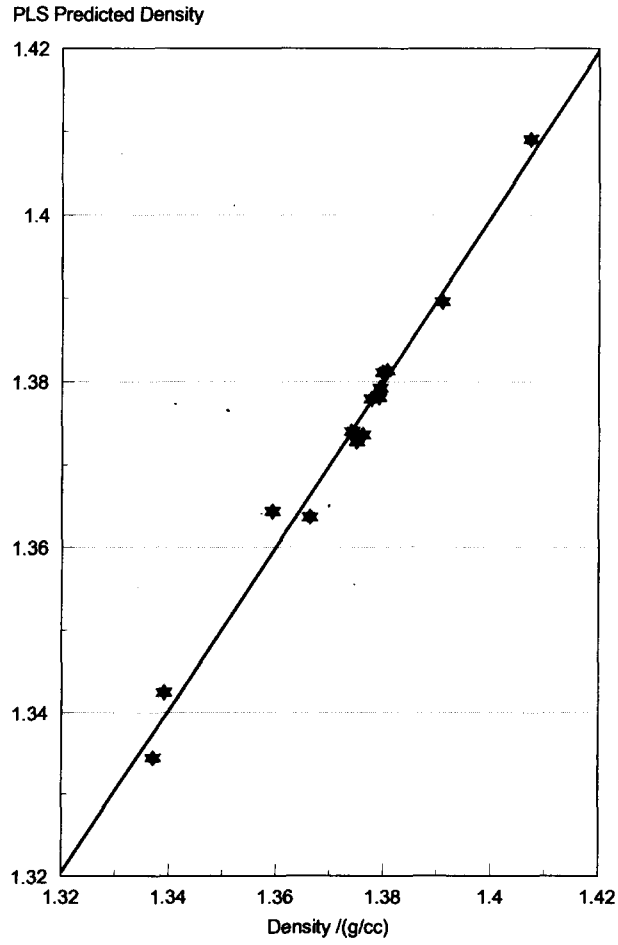


**Figure 11** Cross-validation plot obtained from the PLS model of a PET chip sample set; SEP = 0.0022 g $cm^{-3}$

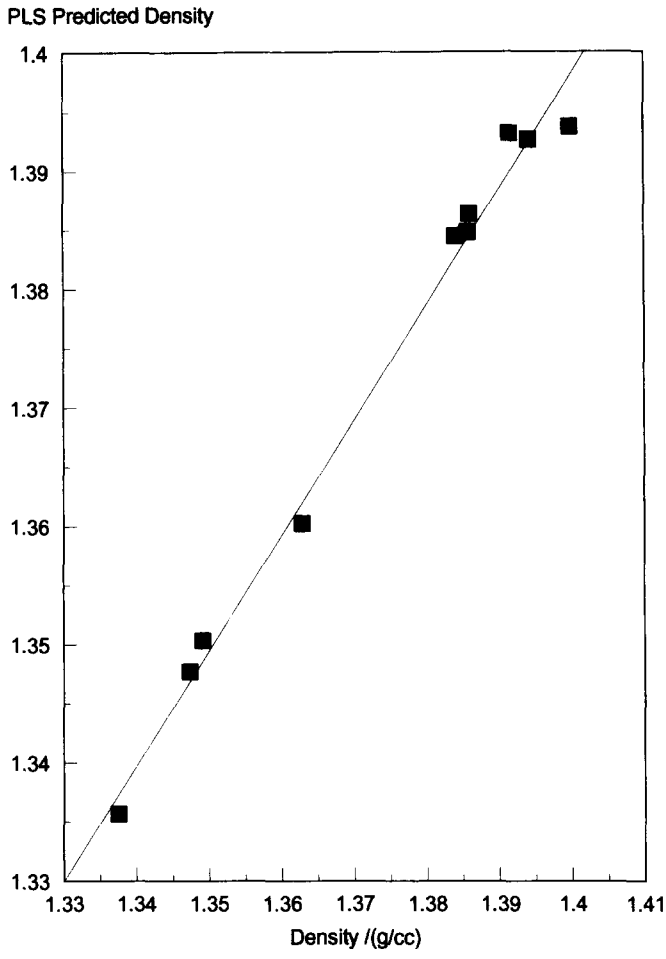


**Figure 12** Cross-validation plot obtained from the PLS model of a PET drawn film sample set; SEP = 0.0023 g cm$^{-3}$

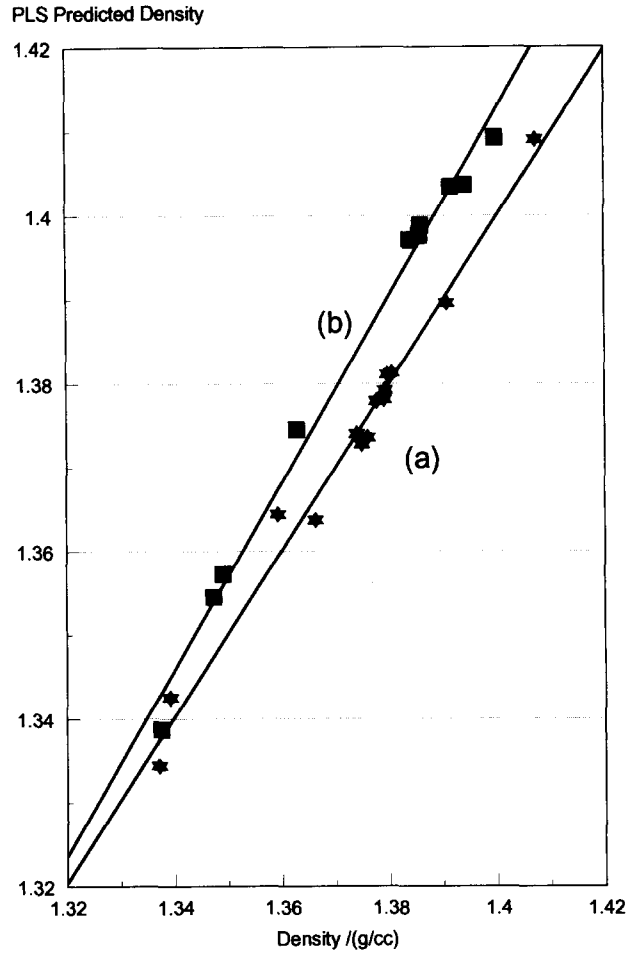


**Figure 13** Result of using the 'chip only' PLS model to attempt to predict densities of film samples: (a) chip predictions (∗); (b) film predictions (■). The model predicts anomalously high values for the film densities, in the same way that the univariate calibrations fail (see *Figures 3* and *4*). A good PLS model needs both chip and film calibration standards, e.g. *Figure 9*

actually sensitive to intramolecular conformation, and so the PLS calibration might fail if applied to highly oriented samples which have been prepared in an 'amorphous' state[4]; fortunately this is not the usual situation with PET samples of practical interest.

## CONCLUSIONS

*FT*(n.i.r.) Raman spectroscopy and Chemometrics analysis were used to reexamine correlations previously observed between conventional Raman spectra and the density of PET samples. N.i.r. Raman spectroscopy is advantageous in reducing the fluorescence which occurred on annealing PET samples. HCA and PCA proved useful in classifying samples, particularly in distinguishing between oriented and isotropic PET, and PCA indicated that the bands at ~1730, 1094, 997, and 860 cm$^{-1}$ were most strongly affected by the changes occurring on annealing the PET. However, the degree of molecular orientation also influenced these bands. Significantly, the 1615 cm$^{-1}$ ring mode, which is known to be sensitive to orientation, also proved important in differentiating the chips, although it is not clear at this time what is influencing the changes in this band with these samples. It is obvious that factors other than density or orientation differentiate the chip spectra under PCA treatment, and possible differences in sample morphology (conformation chain packing) or degradation may be important. More work is needed to elucidate these effects.

PLS modelling was very successful in producing a calibration for the density of both isotropic and anisotropic samples; an SEP (cross-validated) of 0.0024 g cm$^{-3}$ was obtained. Most importantly, the PLS model for the full sample set was almost as accurate as individual models for chip or film sample sets in isolation; this was in distinct contrast to univariate calibrations based on the carbonyl stretching bandwidth or the 1094 cm$^{-1}$ band intensity, where separate calibrations for chip and drawn film samples have to be used. The PLS model utilized most strongly the bands at 1730, 1094, and 860 cm$^{-1}$ in predicting the sample densities.

In conclusion, we have shown that PLS modelling is a powerful tool for decoupling the effects of orientation and crystallinity to produce a model for measuring PET density from Raman data, irrespective of the degree of orientation, and that PCA can provide valuable qualitative information for differentiating samples and correlating spectral changes with physico-chemical properties.

## ACKNOWLEDGEMENTS

The authors would like to thank ICI plc for permission to publish this work. We gratefully acknowledge Dr P. Wilkes (ICI Films) for supplying the uniaxially oriented film samples.

## REFERENCES


1 Manley, T. R. and Williams, D. A. *Polymer* 1969, **10**, 339
2 Daubeny, R., Bunn, C. W. and Brown, C. J. *Proc. R. Soc. London* 1954, **A226**, 531
3 Lin, S. B. and Koenig, J. L. *J. Polym. Sci. Polym. Phys. Edn* 1982, **20**, 2277
4 Adar, F. and Noether, H. *Polymer* 1985, **26**, 1935
5 Melveger, A. *J. Polym. Sci. (A-2)* 1972, **10**, 317
6 Chalmers, J. M., Croot, L., Eaves, J. G., Everall, N., Gaskin, W. F., Lumsdon, J. and Moore, N. *Spectrosc. Int. J.* 1990, **8**, 13
7 Stokr, J., Schneider, B., Doskocilova, D., Lovy, J. and Sedlacek, P. *Polymer* 1982, **23**, 714
8 Hartigan, J. A. 'Clustering Algorithms', Wiley, New York, 1975
9 Massart, D. L., Vandeginste, B. G. M., Dening, S. N., Michotte, Y. and Kaufman, L. 'Chemometrics: a Textbook', Elsevier, Amsterdam, 1988
10 Martens, H. and Naes, T. 'Multivariate Calibration', Wiley, New York, 1989
11 Haaland, D. M. and Thomas, E. V. *Anal. Chem.* 1988, **60**, 1193
12 Everall, N. and Lumsdon, J. *Vibrational Spectrosc.* 1991, **2**, 257
13 Petty, C. J. *Vibrational Spectrosc.* 1991, **2**, 263
14 Schrader, B., Hoffmann, A., Simon, A. and Sawatzki, J. *Vibrational Spectrosc.* 1991, **1**, 239
15 Jarvis, D. A., Hutchinson, I. J., Bower, D. I. and Ward, I. M. *Polymer* 1980, **21**, 41


## APPENDIX

### *PET sample preparation and densities*

**Table 1** Chip samples

| Sample code | Density (g ml$^{-1}$) | Preparation |
|---|---|---|
| ob00 | 1.3358 | Not annealed |
| ob25 | 1.3371 | 16 min at 100°C |
| ob21 | 1.3391 | 30 min at 100°C |
| ob23 | 1.3593 | 1 h at 100°C |
| ob24 | 1.3663 | 2 h at 100°C |
| ob43 | 1.3740 | 31 min at 120°C |
| ob41 | 1.3749 | 1 h at 120°C |
| ob42 | 1.3760 | 2 h at 120°C |
| ob64 | 1.3777 | 14 min at 140°C |
| ob62 | 1.3791 | 1 h at 140°C |
| ob74 | 1.3793 | 15 min at 150°C |
| ob73 | 1.3798 | 1 h at 150°C |
| ob72 | 1.3806 | 2 h at 150°C |
| ob228 | 1.3908 | 10 h at 150°C |
| ob521 | 1.4073 | 24 h at 150°C |

**Table 2** Uniaxially drawn film samples

| Sample code | Density (g ml$^{-1}$) | Forward draw ratio |
|---|---|---|
| PET 52 | 1.3375 | 2.5 |
| PET 51 | 1.3473 | 3.0 |
| PET 50 | 1.3491 | 3.5 |

**Table 3** Biaxially drawn film samples[a]

| Sample code | Density (g ml$^{-1}$) | Temperature (°C) | Time (min) |
|---|---|---|---|
| PET 43 | 1.3628 | 40 | 1.5 |
| PET 44 | 1.3840 | 180 | 0.5 |
| PET 45 | 1.3858 | 180 | 1.0 |
| PET 46 | 1.3860 | 180 | 1.5 |
| PET 47 | 1.3915 | 210 | 0.5 |
| PET 48 | 1.3941 | 210 | 1.0 |
| PET 49 | 1.3998 | 230 | 1.0 |

[a]These films all had a forward draw ratio of 3.4 and a sideways draw ratio of 3.5

All film samples were produced on a semi-technical continuous film line at the ICI Wilton Research Centre. The uniaxial films were not heat set.